Full-Polarimetric Analysis of MERIC Air Targets Data

C. Titin-Schnaider, P. Brouard
ONERA
Chemin de la Hunière et des Joncherettes
91120 Palaiseau
France

Cecile.Titin-Schnaider@onera.fr , Philippe.Brouard@onera.fr

ABSTRACT

This paper addresses the detailed analysis of full polarimetric radar images, obtained from real data, by using the Polarimetry theory parameters.

The experimental ground based radar station MERIC has been designed at ONERA to perform full polarimetric measurements on non-cooperative in flight airplanes.

The first promising results of an analysis carried out from a MERIC full-polarimetric ISAR image of a liner are presented.

1.0 INTRODUCTION

The theory of polarization has been studied [1] for several decades. However, its implementation has been delayed while waiting for technological progress. At present, experimental high resolution radar can provide full-polarimetric data with the required magnitude and especially phase accuracy.

Some full polarimetric airborne SAR radars have already been developed. Full-polarimetric SAR images analysis (produced from RAMSES data, for example), has shown promising results regarding the vegetation classification and the analysis of motionless ground targets.

For In-flight target studies, 2D-ISAR radar imaging is a well-established method giving the reflectivity distribution of target scatterers. Full-polarimetric ISAR imaging will be introduced and discussed. It will be shown that Polarimetry provides additional information about scatterers electromagnetic behaviour.

The full-polarimetric ground based radar station MERIC has been designed to measure in-flight targets [4], in order to create full-polarimetric data base. The analysis of a civilian aircraft is presented to illustrate Polarimetry potentiality.

2.0 ISAR FULL-POLARIMETRIC IMAGING

2.1. Radar images

Radar targets can be split into two main classes depending on how elementary mechanisms add in the resolution cell.

- If they add incoherently, scattering mechanisms are represented by random variables and the statistical (or general) theory of polarization is applicable. This is the case for large natural areas like forests, fields, meadows....

Paper presented at the RTO SET Symposium on "Target Identification and Recognition Using RF Systems", held in Oslo, Norway, 11-13 October 2004, and published in RTO-MP-SET-080.

- If they add coherently, electromagnetic scatterings are coherent and the deterministic theory of polarization is applicable. This is mainly the case for man-made or artificial targets like aeroplanes, trucks, railways ... Radar images of these targets are characterized by a small number of bright scattering centres.

2.2. Point Object Model

- A common assumption for radar artificial radar targets is the 'Point Object Model' (POM). According to this model, any target is described by a collection of isotropic point scatterers.
- Polarimetric measurement give access to the target backscattered matrix [S].

In the POM frame, this matrix can be represented by a sum on N elementary scattering matrices [s_i], phase shifted according to the scatterers locations $\vec{x}_i$:

$$[S](\vec{k}) = \sum_{i=1,N} [s_i]\, e^{j2\vec{k}\cdot\vec{x}_i}$$

where $\vec{k} = \frac{2\pi f}{c}\frac{\vec{r}}{r}$ is the wave vector depending on frequency f and incidence angle.

For any radar system, the image $[I](\vec{x})$ is obtained through a Fourier Transform:

$$[I](\vec{x}) = \int [S](\vec{k})\, e^{-j2\vec{k}\cdot\vec{x}}\, d\vec{k}$$

Assuming the elementary matrices [s_i] do not vary with frequency and orientation, the image is given by:

$$[I](\vec{x}) = \sum_{i=1,N} [s_i]\, \delta(\vec{x} - \vec{x}_i)$$

where $\delta(\vec{x})$ is the Dirac distribution.

In practice, measurements are recorded over a limited frequency bandwidth and over a bordered incidence domain. Therefore, the Point Spread Function (PSF) $G(\vec{x} - \vec{x}_i)$ replaces the Dirac distribution:

$$[I](\vec{x}) = \sum_{i=1,N} [s_i]\, G(\vec{x} - \vec{x}_i)$$

This equation shows that the resulting image can be considered as the complex sum of each point scatterer image. Bright scattering centres are no longer point centres. They have a stretch in space characterized by the PSF. The same elementary scattering matrix is associated with all pixels in the vicinity of a point scatterer with a strength given by the PSF. If the scatterers are far enough from each other, their PSF do not interfere and the true elementary matrices $[s_i]$ are obtained at locations $\vec{x}_i$. A target is therefore described by a set of point scatterers whose elementary scattering matrices and locations are known.

In practice, the scattering matrix of a given scatterer is always more or less distorted by the scattering matrix of the other scatterers. The higher is the resolution, the smaller is the PSF and the less distorted are the elementary scattering matrices.

A 2D ISAR image is a projection of the 3D scatterer distribution onto a 2D plane. Some different scatterers can then be confused. This problem increases for the 1D representation: a range profile being the

projection on the line of sight of the 3D distribution of scatterers. So in this case a larger number of scatterers can be mixed together.

2.3 ISAR imaging

To build the ISAR image of a moving target with the required transversal resolution, the radar has to track the target in order to acquire measurements during a sufficiently long duration. Each complex range profile thus acquired must be aligned with the preceding profile using a complex correlation method.

Phase distortion due to the translation motion of the moving target is compensated using the DSA (Dominant Scatterer Algorithm) method. The principle of this method is to select the bright scatterer showing the least amplitude variation as a reference point,

At radar wavelengths, the returned signal is dominated by backscattering from features like corners, edges and surface discontinuities… The objective of radar classification based on classical ISAR imaging is to consider rather the locations and RCS level of scatterers than target shape. Full polarimetric radar data makes it possible to also use electromagnetic mechanisms creating the scatterers.

3.0 POLARIMETRIC PARAMETERS

The nature of deterministic mechanisms can be characterised by several sets of polarimetric parameters. These sets are globally equivalent. However their sensitivity to electromagnetic properties can be different.

3.1. Sets of polarimetric parameters

It is well known that deterministic mechanisms are described by a 2 by 2 complex matrix: the scattering matrix. Under the reciprocity postulate and given its absolute phase is ineffective for describing the physical mechanism, it depends on five independent parameters. Several sets of parameters have been proposed in the literature:

- The Fork parameters set:

According to [1] the back-scattering matrix of any deterministic mechanism can be mathematically represented by several operators:

$$[S] = e^{-i\psi[\sigma_0]} e^{-i\tau[\sigma_2]} [S_d] e^{-i\tau[\sigma_2]} e^{i\psi[\sigma_0]}$$

where: $[S_d] = \mu e^{i2\nu} \begin{bmatrix} 1 & 0 \\ 0 & (tg\gamma)^2 e^{-i4\nu} \end{bmatrix}$ and where the four Pauli matrices are noted $[\sigma_j]$, $j = 0,3$.

It depends on the five Polarization Fork angles: $\psi, \tau, \gamma, \nu, \mu$ The variation ranges of the Polarization Fork parameters are as follows:

$$-\pi/2 < \psi < \pi/2 \quad -\pi/4 < \tau < \pi/4 \quad -\pi/4 < \nu < \pi/4 \qquad 0 < \gamma < \pi/4$$

The orientation angle ψ gives the tilt of the target versus the horizontal polarization, in the plane perpendicular to the radar line of sight. The symmetry angle τ indicates the symmetry rate versus an axis or a plane (if τ is low the scatterer is symmetric and if it is high it is not symmetric). The skip angle ν gives information about the parity of the number of scatterings (if ν is low this number is even, if ν is

high it is odd). The polarizability angle γ provides information about the ability of the scatterer to polarize the waves on a particular polarization (if γ is low the scatterer is polarizing and if γ is high it is not).

- The Huynen parameters set:

This set contains nine real parameters [1]:

the orientation angle ψ and the disoriented (orientation extracted) Muller matrix parameters:

$$2A_0, B_0 + B, B_0 - B, C, D, E, F, G$$

In the deterministic case, these parameters are linked by four relations:

$$2A_0(B_0 + B) = C^2 + D^2 \qquad 2A_0 E = DG \qquad 2A_0(B_0 - B) = G^2 \qquad 2A_0 F = CG$$

All these parameters are homogeneous to a power. The span is an invariant quantity (independent of any polarization base change) representing the total RCS back-scattered by the target:

$$span = |S_{hH}|^2 + |S_{hV}|^2 + |S_{vH}|^2 + |S_{vV}|^2 = 2A_0 + (B_0 - B) + (B_0 + B)$$

A feature vector valid for identification (independent of total power information) is obtained through the unit span normalization: $2A_0 + (B_0 + B) + (B_0 - B) = 1$

The Huynen parameters can be written [1] as a function of the Fork parameters. Then, it is easy to maximise each Huynen parameter. Figure 1 a, b, c, d, e, f, g contains the combs obtained when parameters $2A_0, B_0 + B, B_0 - B, C, D\ E, F, G$ are respectively maximised. One can notice that maximising any generator parameter $2A_0$, $B_0 + B$ and $B_0 - B$ leads to a comb with only one peak (1a, b, c). The maximum of any other parameter corresponds to a comb with three equal peaks (1d, e, f, g, h).

Therefore, the unit span constraint leads to a set of eight characteristic feature combs (figure 1) with either one peak (equal to 1) or three equal peaks (equal to ½). The very good continuity from one feature comb to another is an important advantage for a classification algorithm based on correlation between measured and reference combs.

In practice, most of the analysed scattering centres are symmetrical ($\tau \approx 0$). Therefore, we often have: $E = F = G = 0$.

Only the five first combs of figure 1 are frequently found. The main electromagnetic mechanisms are:

- Specular reflection on a smooth surface locally spherical or on a plate. In this case the dominating parameter is $2A_0$ (figure 1a).

- Scattering on a sharp edge or on a long and thin wire described by a comb looking like figure 1d. A maximum value of parameter C corresponds to three equal peaks for $2A_0$, $B_0 + B$ and C.

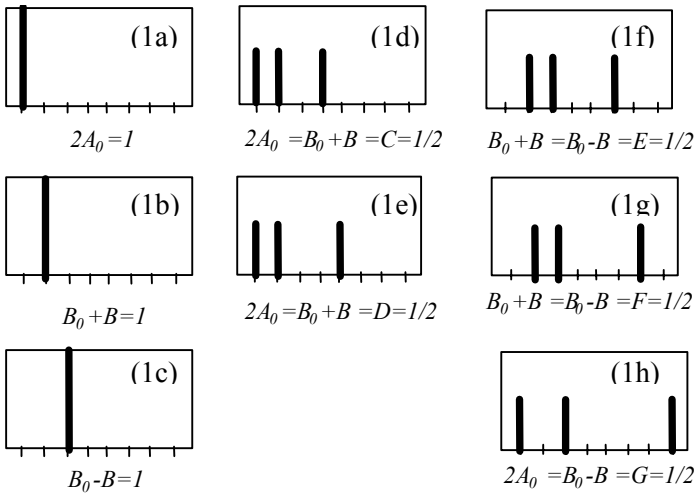

Figure 1 : the eight characteristic combs

- A difference between the two local curvatures is characterized by an increase of parameter D. A maximum value of D corresponds to three equal peaks for $2A_0$, B_0+B and D (figure 1e). It describes the quarter-wave dephasors according the sign of D.
- The maximum of parameter F is described by three equal peaks (figure 1g). It corresponds to helices according the sign of F.

4.0 POLARIMETRIC ANALYSIS OF AN AIRCRAFT

A specific software has been designed at ONERA to assist polarimetric analysis of full-polarimetric radar images. In particular, it can be used to calculate and show the image of any polarimetric parameter for any selected area. Several recognition methods can be used to improve the analysis (based on a comparison between either scattering matrices or combs of Huynen parameters…).

As an example, results obtained from a full-polarimetric analysis of a civilian aircraft measured by MERIC radar, are presented. The chosen aircraft is a Mac Donnel Douglas MD 82 in take-off phase. A photo (figure 2) gives an idea of the aircraft presentation with regards to the radar during the measurements.

The RCS images of the four r(eceive)/T(ransmit) polarizations hH, hV, vH and vV are given in figure 3. About ten main bright spots appear very clearly. The great similarity between the hV and vH images (in accordance with the reciprocity postulate) can be seen. These four images show that co and cross polarized images must be taken into account.

The bright spot areas are defined by selecting all pixels with span greater than a given level. In figures 4 to 7, the eliminated pixels are indicated in light green.

Images of the Huynen parameters 2A0 (Figure 4) and B0+B (Figure 5) show that these parameters are very discriminating. The higher values (in warm colours) of parameter 2A0 indicate the surface mechanisms locations. On the other hand, the higher values (in warm colours) of parameter B0+B show the double-bounce areas. The analysis can be refined by calculating the comb of Huynen parameters for various selected variable size areas. This kind of analysis allows us to identify numerous scatterers.

Automatic recognition algorithms can be applied on each pixel to obtain a classified image: a set of mechanisms are stored in the reference memory. The most likely mechanism of the reference memory

(according to an appropriate rule of comparison) is allocated to each pixel. The algorithm can be based equally well on either a comparison between scattering matrices [2] or on a comparison between Huynen parameters combs. A classified image is presented on the right part of Figure 6 and Figure 7.

The mechanisms are represented by a specific colormap: Surface mechanism ("S") in blue, Double-bounce or dihedral type mechanisms ("Dd") in red. The dipole type mechanisms indicating lengthened targets ("Dp") are referenced in yellow. Positive or negative quarter-wave dephasors devices ("Q$\pm$") in purple and mauve colours. Two intermediate mechanisms are introduced: cylinder ("C") between surface mechanism and dipole; lengthened dihedral corner ("DdL") between dihedral and dipole. Among non-symmetrical targets, the right and left helices ("H$\pm$") are associated with white and black. The light grey ("X") or dark grey ("Y") colours indicate symmetric and non-symmetric unrecognized mechanisms respectively.

Numerous scatterers generating surface (right part of figure 6) and double-bounce mechanisms (right part of figure 7) have been recognized. On the left part of figures 6 and 7, identified mechanisms locations are indicated.

Surface scatterers are identified in blue and green on figure 6. They are located on:

- the end of the tail flat (1),
- the left (2) and right (3) engines,
- the fuselage (4), (6), (8),
- the end of the wing (5),
- the opposite part of the fuselage (7).

Double-bounces are identified on figure 7. They indicate the following interactions:

- rudder - right part of the horizontal tail flat (1),
- rudder - left part of the horizontal tail flat (2),
- back of right engine (3),
- trailing edge flap control systems casing - underside of right wing (4),(5),(6),
- fuselage - back of the right wing (7),
- fuselage - front of the right wing (8),
- fuselage – antennas (9),(10), (11).

5.0 CONCLUSION

Like all man-made targets, aircraft radar images are characterized by a collection of bright scatterers. Conventional 2D-ISAR imagery can determine their location and RCS. Full-polarimetric ISAR imaging provides access to extra information about the electromagnetic mechanisms that creates them.

This study, carried out on real data provided by MERIC full-polarimetric radar, shows that a lot of information can be obtained using Polarimetry. Mechanisms like specular reflection on plate or on curved surface, edge diffraction, double-reflection, surface waves, surface discontinuity…. can be recognized.

Future measurements that will be provided by MERIC station can be used to build a full-polarimetric database of air targets. From this database, suitable methods of automatic target recognition will be

proposed and tested on fully or partially real polarimetric data, in order to assess the usefulness of Polarimetry.

6.0 REFERENCES

[1] Huynen J.R., "Phenomenological theory of radar targets". Phd Thesis, 1970

[2] Cameron W.L., Leung L.K., "Identification of elemental polarimetric scatterer responses in high-resolution ISAR and SAR signature measurements", Second international workshop on radar polarimetry, Nantes, September 1992.

[3] Titin-Schnaider C., Dreuillet P., "Analyses polarimétriques haute résolution de mesures de cibles radar en laboratoire", JIPR, Nantes, mars 95

[4] Titin-Schnaider C., Attia S.," Calibration of the MERIC Full-Polarimetric Radar: theory and implementation ". Aerospace Science and Technology – August 2004

7.0 GLOSSARY

MERIC : Moyen Expérimental pour la Reconnaissance et l'Identification des Cibles

RAMSES : Radar Aéroporté Multi Spectral d'Etude des Signatures

Figure 2 : MD82 picture in taking off phase

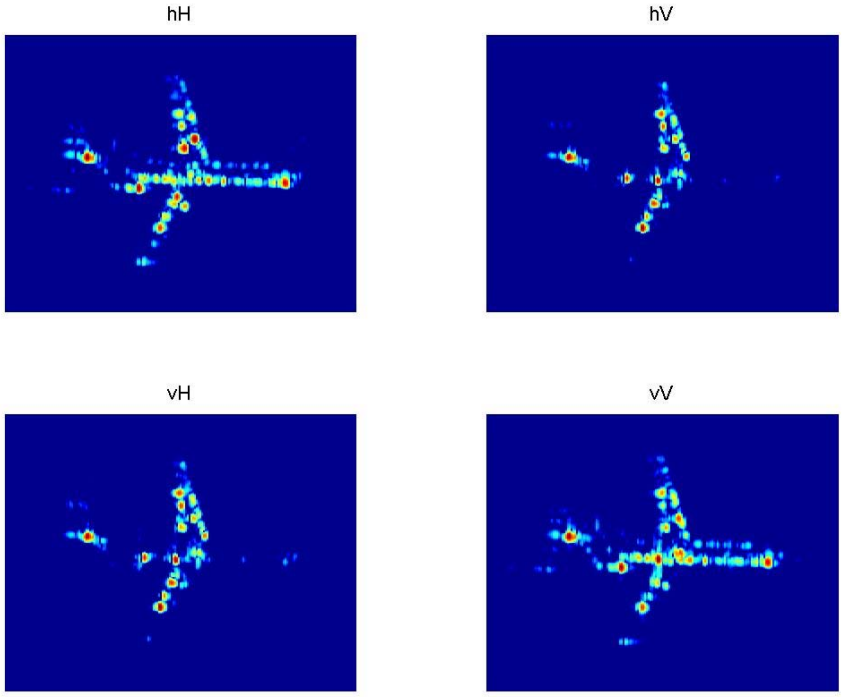

Figure 3 : four-polarimetric RCS ISAR images

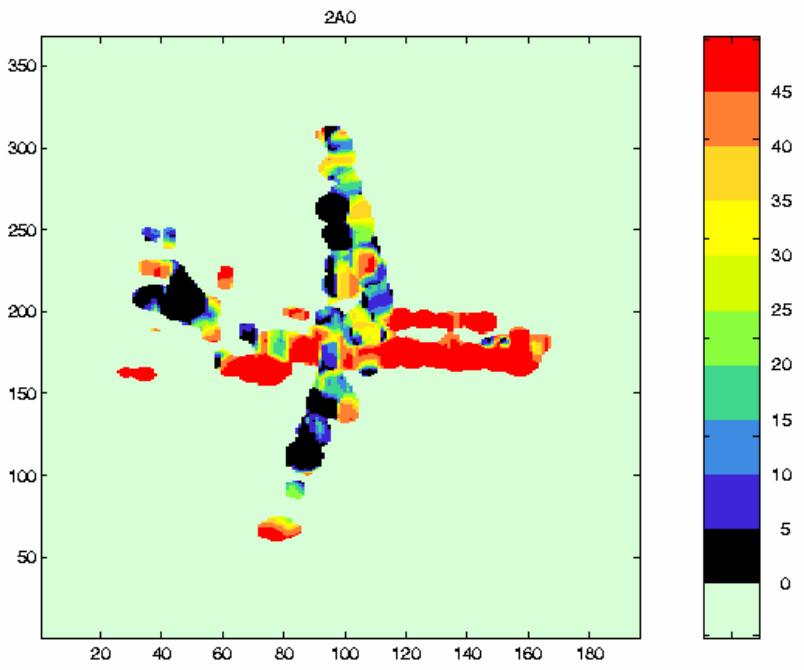

Figure 4 : 2A0 parameter image

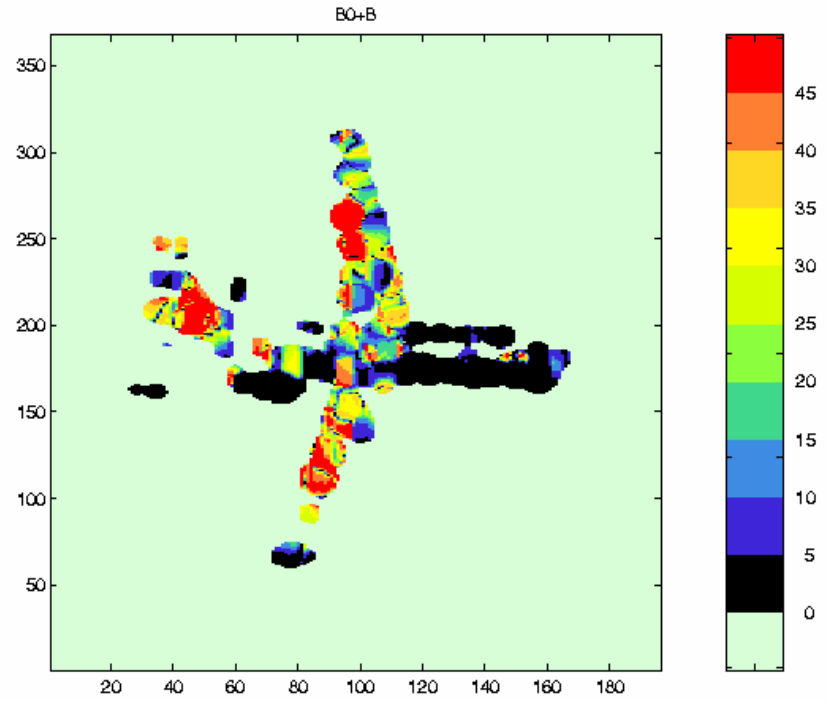

Figure 5 : B0+B parameter image

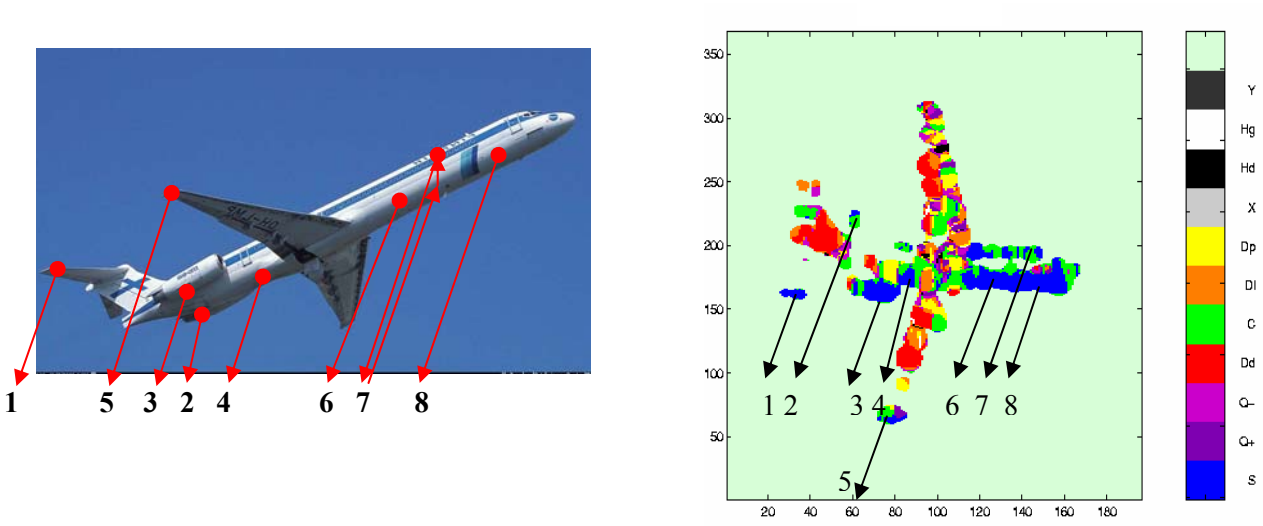

Figure 6 : surface mechanisms analysis

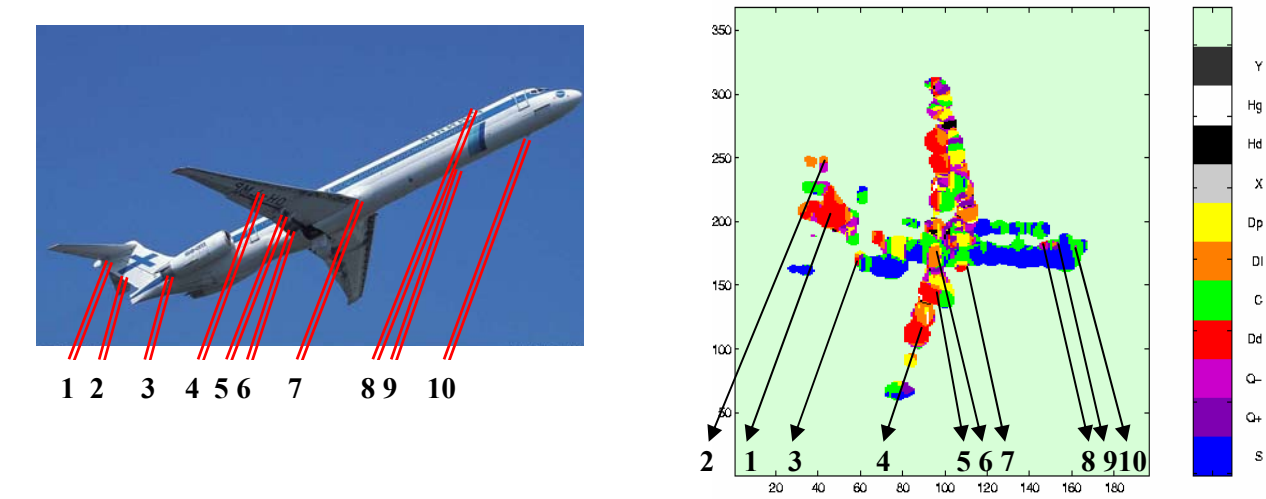

Figure 7 : double-bounce mechanisms analysis